

Deconfinement and freezeout boundaries in equilibrium thermal models

Abdel Nasser Tawfik*

*Nile University, Egyptian Center for Theoretical Physics (ECTP),
Juhatna Square of 26th-July-Corridor, 12588 Giza, Egypt and
Goethe University, Institute for Theoretical Physics (ITP),
Max-von-Laue-Str. 1, D-60438 Frankfurt am Main, Germany*

Muhammad Maher, A. H. El-Kateb, and Sara Abdelaziz

Helwan University, Faculty of Science, Physics Department, 11795 Ain Helwan, Egypt

(Dated: August 2, 2019)

In different approaches, the temperature - baryon density plane of QCD matter is studied for deconfinement and chemical freezeout boundaries. Results from various heavy-ion experiments are compared with the recent lattice simulations, the effective QCD-like Polyakov linear-sigma model, and the equilibrium thermal models. Along the entire freezeout boundary, there is an excellent agreement between the thermal model calculations and the experiments. Also, the thermal model calculations agree well with the estimations deduced from the Polyakov linear-sigma model (PLSM) [1]. At low baryonic density or high energies, both deconfinement and chemical freezeout boundaries are likely coincident and therefore the agreement with the lattice simulations becomes excellent as well, while at large baryonic density, the two boundaries become distinguishable forming a phase where hadrons and quark-gluon plasma likely coexist.

PACS numbers: 12.40.Ee, 12.40.Yx, 05.70.Ce

Keywords: Statistical models, Hadron mass models and calculations, Thermodynamic functions and equations of state

I. INTRODUCTION

Strongly interacting matter under extreme conditions is characterized by different phases and different types of the phase transitions [2]. The hadronic phase, where stable baryons build up a great part of the Universe and the entire everyday life, is a well known phase. At high temperatures and/or densities, other phases appear. For instance, at temperatures of a few MeV, chiral symmetry restoration and deconfinement transition take place, where quarks and gluons are conjectured to move almost freely within colored phase known as the quark-gluon plasma (QGP) [3]. At low temperatures but large densities, the hadronic (baryonic) matter forming compact interstellar objects such as neutron stars is indubitably observed in a conventional way and very recently gravitational waves from neutron star mergers have been detected, as well [4]. At larger densities, extreme interstellar objects such as quark stars are also speculated. In lattice quantum chromodynamics (QCD), different orders of chiral and deconfinement transitions have been characterized, especially at low baryon densities.

The program of heavy-ion collision experiments dates back to early 1980's. Past (AGS, SIS, SPS), current (RHIC, LHC), and future facilities (FAIR, NICA) help in answering essential questions about the thermodynamics of the strongly interacting matter and in mapping out the temperature - baryon density plane [3]. The unambiguous evidence on the formation of QGP is an example of a great imperial achievement [5, 6]. The colliding nuclei are conjectured to form a fireball that cools down by rapid expansion and finally hadronizes into individual uncorrelated hadrons. The present script focuses on the temperature - baryon density plane, concretely near the hadron-QGP boundaries, in framework of equilibrium thermal model [7]. To this end, we put forward a basic assumption that both directions, hadron-QGP and QGP-hadron phase are quantum-mechanically allowed [8]. In other words, the picture drawn so far seems in fundamental conflict with the time arrow. The concept of arrow of time prevents the reverse direction, especially if the change in the degrees of freedom or entropies aren't following the causality principle; second law of thermodynamics. That statistical thermal approaches

*Electronic address: tawfik@itp.uni-frankfurt.de

work well near to both deconfinement and chemical freezeout boundaries [3, 9] could be understood in the light of the thermal nature of an arbitrary small part of the highly entangled fireball states. Following the Eigenstate Thermalization Hypothesis [8, 10], the corresponding probability distribution of the projection of these states remains thermal. We follow the line that the thermal models reproduce well the particle yields and the thermodynamic properties of the hadronic matter including the chiral and freezeout temperatures. We compare our calculations with reliable lattice QCD simulations, an effective QCD-like approach, and available experimental results.

The present script is organized as follows. In section II approaches for deconfinement and freezeout boundaries in equilibrium thermal models are introduced. The results are discussed in section III. Section IV is devoted to the conclusions and outlook.

II. EQUILIBRIUM THERMAL MODELS

It was conjectured that the formation of the hadron resonances follows the bootstrap picture, i.e. the hadron resonances or the fireballs are composed of further resonances or fireballs, which in turn are consistent of lighter resonances or smaller fireballs and so on [11, 12]. The thermodynamic quantities of such a system can be deduced from the partition function $Z(T, \mu, V)$ of an ideal gas. In a grand canonical ensemble, this reads [3, 13–17]

$$Z(T, V, \mu) = \text{Tr} \left[\exp \left(\frac{\mu N - H}{T} \right) \right], \quad (1)$$

where H is Hamiltonian combining all relevant degrees of freedom and N is the number of constituents of the statistical ensemble. Eq. (1) can be expressed as a sum over all hadron resonances taken from recent particle data group (PDG) [18],

$$\ln Z(T, V, \mu) = \sum_i \ln Z_i(T, V, \mu) = V \frac{g_i}{2\pi^2} \int_0^\infty \pm p^2 dp \ln \left[1 \pm \lambda_i \exp \left(\frac{-\varepsilon_i(p)}{T} \right) \right], \quad (2)$$

where the pressure reads $T \partial \ln Z(T, V, \mu) / \partial V$, \pm stands for fermions and bosons, respectively. $\varepsilon_i = (p^2 + m_i^2)^{1/2}$ is the dispersion relation and λ_i is the fugacity factor of i -th particle [3],

$$\lambda_i(T, \mu) = \exp \left(\frac{B_i \mu_b + S_i \mu_s}{T} \right), \quad (3)$$

where $B_i(\mu_b)$ and $S_i(\mu_s)$ are baryon and strangeness quantum numbers (their corresponding chemical potentials) of the i -th hadron, respectively. From phenomenological point of view, the baryon chemical potential μ_b can be related to the nucleon-nucleon center-of-mass energy $\sqrt{s_{NN}}$ [19]

$$\mu_b = \frac{a}{1 + b\sqrt{s_{NN}}}, \quad (4)$$

where $a = 1.245 \pm 0.049$ GeV and $b = 0.244 \pm 0.028$ GeV⁻¹. The number and energy density, respectively, can be derived as

$$n_i(T, \mu) = \sum_i \frac{\partial \ln Z_i(T, V, \mu)}{\partial \mu_i} = \sum_i \frac{g_i}{2\pi^2} \int_0^\infty p^2 dp \frac{1}{\exp \left[\frac{\mu_i - \varepsilon_i(p)}{T} \right] \pm 1}, \quad (5)$$

$$\rho_i(T, \mu) = \sum_i \frac{\partial \ln Z_i(T, V, \mu)}{\partial (1/T)} = \sum_i \frac{g_i}{2\pi^2} \int_0^\infty p^2 dp \frac{-\varepsilon_i(p) \pm \mu_i}{\exp \left[\frac{\mu_i - \varepsilon_i(p)}{T} \right] \pm 1}. \quad (6)$$

Likewise, the entropy and other thermodynamic quantities can be derived straightforwardly.

Both temperature T and the chemical potential $\mu = B_i \mu_b + S_i \mu_s + \dots$ are related to each other and to $\sqrt{s_{NN}}$ [3]. As an overall thermal equilibrium is assumed, μ_s is taken as a dependent variable to be estimated due to the strangeness conservation, i.e. at given T and μ_b , the value assigned to μ_s is the one assuring $\langle n_s \rangle - \langle n_{\bar{s}} \rangle = 0$. Only then, μ_s is combined with T and μ_b in determining the thermodynamic quantities, such as the particle number, energy, entropy, etc. The chemical potentials related to other quantum charges, such as the electric

change and the third-component isospin, etc. can also be determined as functions of T , μ_b , and μ_s and each of them must fulfill the corresponding laws of conservation.

This research intends to distinguish between deconfinement and freezeout boundaries in equilibrium thermal models. The latter is characterized by T_χ and μ_b , which are conditioned to one of the universal freezeout conditions [20], such as constant entropy density normalized to T_χ^3 [21, 22], constant higher-order moments of the particle multiplicity [23, 24], constant trace anomaly [25] or an analogy of the Hawking-Unruh radiation [26]. The experimental estimation for T_χ and μ_b , as shown in Fig. 1 proceeds through statistical fits for various particle ratios calculated in statistical thermal models. The former, the deconfinement transition, is conditioned to line-of-constant-physics, such as constant energy density, ρ [27]. The inclusion of the strange quarks seems to affect the critical temperatures, as these come up with extra hadron resonances and thier thermodynamic contributions, where the mass of strange quarks is of the order of the critical temperature.

III. RESULTS

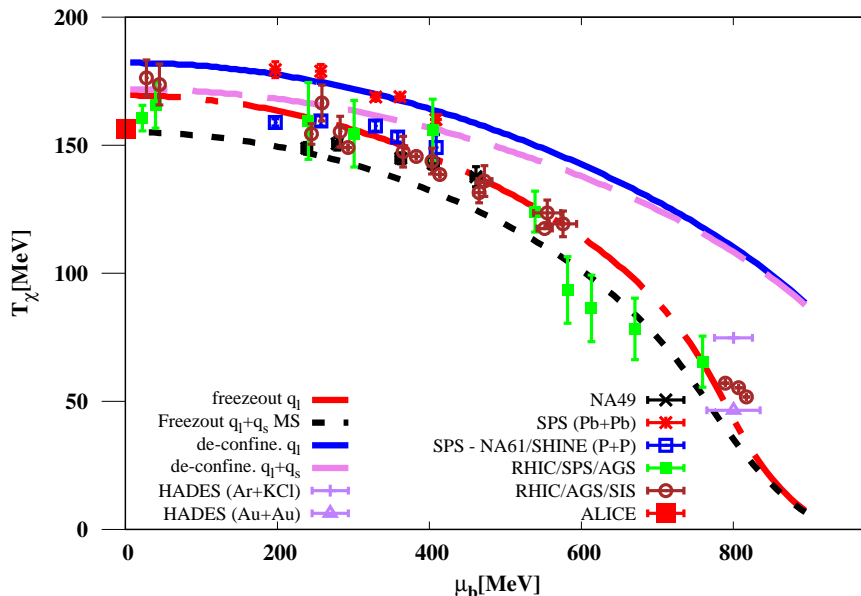


Fig. 1: The freezeout and deconfinement parameters T_χ and μ_b as deduced from different experimental results (symbols with errorbars) are combined with each other and confronted with the thermal model calculations for the freezeout (dot-dashed and dashed curves) and deconfinement parameters (solid and long-dashed curves) with and without strange quarks.

Figure 1 depicts the freezeout and deconfinement parameters T_χ and μ_b as determined from different experimental results (symbols with errorbars) are combined with each others and compared with the thermal model calculations. The latter take into account both freezeout (dot-dashed and dashed curves) and deconfinement boundaries (solid and long-dashed curves) with and without strange quarks.

With the experimental results we mean the parameters obtained when measured particle yields and/or ratios are fitted to calculations based on statistical thermal models, in which the parameters T_χ and μ_b are taken as independent variables. μ_b can directly be fixed at given center-of-mass energy $\sqrt{s_{NN}}$, Eq. (4). For the freezeout parameters T_χ , μ_b , μ_s , etc. the thermodynamic quantities which fulfill one of the freezeout conditions reviewed in refs. [16, 20]. Conditions for deconfinement phase transitions have been discussed in refs. [16, 27], line-of-constant-physics, such as constant energy density with varying μ_b , μ_s , $\sqrt{s_{NN}}$, etc.

It is obvious that both sets of parameters seem identical, especially at low μ_b or high $\sqrt{s_{NN}}$. At large μ_b or low $\sqrt{s_{NN}}$, the difference between the temperatures of freezeout and deconfinement becomes larger. Such a difference would be understood based on the assumption that the chemical freezeout takes place very late after the phase of hadronization. The latter is QCD confinement transition. Its order as simulated in recent lattice

QCD is a likely crossover, i.e. there a wide range of temperatures within which QGP hadronizes or hadrons go through QGP. The time span becomes longer with the increase in μ_b or the decrease in $\sqrt{s_{NN}}$. The conjecture of the existence of a mixed phase is probably another possibility. In this phase, both types of degrees of freedom, hadrons and QGP, live together until the system goes through deconfinement to colored QGP or finally entirely freezes out to uncorrelated colorless hadrons.

The co-existence of different QCD phases was discussed in literature, for instance [28, 29]. The mixed QCD phases can be formed in macroscopic, mesoscopic, and microscopic mixture. As shown in Fig. 1, these mixed phases start being produced at $\sqrt{s_{NN}}$ ranging between ~ 5 and ~ 12 GeV, i.e. $\mu_b \simeq 320$ to $\simeq 560$ MeV [29].

For the freezeout parameters, it is apparent that the agreement between the thermal model calculations and the experimental results is very convincing. This covers the entire μ_b -range and can - among other evidence - be interpreted based on the fact that the freezeout stage is the latest along the temporal evolution of the high-energy collision, where the number of produced particles is entirely fixed. The time elapsed from this stage until the detection process is the shortest comparing to the other QCD processes and therefore it is apparently the most accurate one.

In the present calculations, full quantum statistics [13–17] and hadron resonances with masses up to 2.5 GeV [30] are taken into account. The strangeness degrees of freedom play an important role, especially at low μ_b or high $\sqrt{s_{NN}}$.

For the sake of completeness, we have also checked the same calculations but with the inclusion of a large number of possible missing states [31, 32]. We found that the thermodynamic quantities, especially the ones to which the present script is limited, show sensitivity to these missing states [33]. They are entering our calculations in the same manner as done for the PDG hadrons and resonances.

The missing states are resonances predicted, theoretically, but not yet confirmed, experimentally. Their quantum numbers and physical characteristics are theoretically well known [34]. Basically, they are conjectured to greatly contribute to the fluctuations and the correlations, i.e. higher derivatives of the partition function, estimated in recent lattice QCD simulations [34]. These are the occasions where their contributions becomes unavoidable [31]. Another reason for adding the missing states is that they come up with additional degrees of freedom and considerable decay channels even to the hadrons and resonances which are subject of this present study.

For T_χ and μ_b , a comprehensive comparison between the thermal model calculations (curves) and the results deduced from the lattice QCD simulations (bands) [35, 36] and the Polyakov linear-sigma model (symbols with errorbars) [37] is presented in Fig. 2. Within their statistical and systematic certainties, there is an excellent agreement between the lattice QCD simulations (bands) [35, 36] and the Polyakov linear-sigma model (symbols) [37]. The reason why the lattice QCD simulations are limited to $\mu_q/T_\chi \leq 1$ is the so-called sign problem and the difficulties which arise because of the importance of sampling becomes no longer possible. There are various attempts to anticipate this limitation; continuation from imaginary chemical potential, reweighting methods, applying complex Langevin dynamics, and Taylor expansions in the quark chemical potential μ_q [38].

We also find an excellent agreement between the thermal model calculations for the chemical freezeout parameters and the predictions deduced from the Polyakov linear-sigma model, especially at $\mu_b \gtrsim 300$ MeV. At lower μ_b , the thermal model calculations seem to slightly overestimate T_χ .

This observed agreement would be taken as an evidence supporting the conclusion that the first-principle calculations likely result in $T_\chi - \mu_b$ plane similar to that of the Polyakov linear-sigma model, especially at large μ_b , where the first-principle calculations are no longer applicable.

It is in order now to highlight a few details of the linear-sigma model, which is much simpler than QCD, but based on QCD symmetries, as well [37, 39]. Originally, it was intended to describe the pion-nucleon interactions and the chiral degrees of freedom. A spinless scalar field σ_a and triplet pseudoscalar fields π_a are introduced in theory of quantized fields to the linear-sigma model, which is a low-energy effective model, in which the generators $T_a = \lambda_a/2$ with Gell-Mann matrices λ_a and the real classical field forming an $\mathcal{O}(4)$ vector, $\vec{\Phi} = T_a(\vec{\sigma}_a, i\vec{\pi}_a)$ are included. The chiral symmetry is explicitly broken by 3×3 matrix field $H = T_a h_a$, where h_a are the external fields. Accordingly, under $SU(2)_L \times SU(2)_R$ chiral transformation, such as $\Phi \rightarrow L^+ \Phi R$, the σ_a sigma fields acquire finite vacuum expectation values, which in turn break $SU(2)_L \times SU(2)_R$ down to $SU(2)_{L+R}$. These transformations produce massive sigma particle and nearly massless Goldstone bosons, the pions. Therefore, the constituent quarks gain masses, as well; $m_q = g f_\pi$, where g is coupling and f_π is the pion decay constant. Also, the fermions can be introduced either as nucleons or as quarks. The σ fields under chiral transformations exhibit the same behaviour as that of the quark condensates and thus, σ can be taken as order parameters for the QCD chiral phase transition.

With the incorporation of the Polyakov-loop potential, Lagrangian of PLSM reads $\mathcal{L} = \mathcal{L}_{\bar{\psi}\psi} + \mathcal{L}_m - \mathcal{U}(\phi, \phi^0, T)$,

where the first term stands for Lagrangian density of fermions with N_c color degrees-of-freedom, the second term gives the contributions of the mesonic fields, and finally the third term represents the Polyakov-loops potential incorporating the gluonic degrees-of-freedom and the dynamics of the quark-gluon interactions, i.e. deconfinement is also incorporated in this chiral model.

The questions which arise now are why PLSM reproduces well the non-perturbative lattice QCD simulations and why the PLSM agrees well with the thermal model calculations, especially for the freezeout boundary? The first question can be directly answered. PLSM incorporates both chiral and deconfinement QCD symmetries. On the other hand, it seems that both types of transitions are nearly coincident, especially at vanishing or small baryon chemical potentials. Within this region, both calculations are in excellent agreement with each others. At high temperatures, both chiral symmetry restoration and deconfinement transition produce almost free quarks and gluons, e.g. QGP. The reliability of the chiral effective model, PLSM, seems crucial, especially where lattice field theory is unavailable or the experimental results are not accessible yet.

The second question about the reasons why PLSM agrees well with the freezeout parameters deduced from the thermal model calculations can be answered as follows. First, at $\mu_b \gtrsim 300$ MeV, where lattice field theory likely suffers from the sign problem, it seems that both chiral and deconfinement boundaries become more and more distinguishable. It might be obvious that the critical temperature of the chiral phase transition would be smaller than that of the deconfinement transition, which in turn differs from the freezeout temperatures. Within these two limits, which should be subject of further studies, a temperature region is created, in which a phase of mixed hadron - QGP likely takes place. Last but not least, the $T_\chi - \mu_b$ plane of the Polyakov linear-sigma model [37] was determined under the condition of constant entropy density normalized to T^3 [20–22], i.e. likely manifesting the freezeout boundary. A future phenomenological study should be conducted in order to find out whether the condition of line-of-constant-physics gives results in agreement with the $T_\chi - \mu_b$ plane for deconfinement.

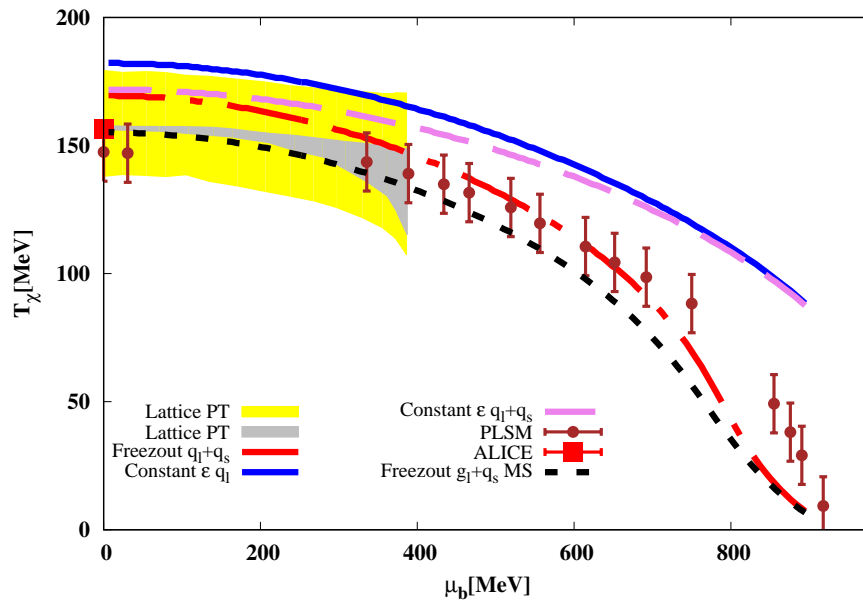


Fig. 2: The same as in Fig. 1 but here comparing between estimations for T_χ and μ_b based on lattice QCD simulations [35, 36] and Polyakov linear-sigma model [37] with the thermal model.

IV. CONCLUSIONS AND OUTLOOK

Among the various phases which take place in the strongly interacting matter under extreme conditions, we focused on the deconfinement and chemical freezeout boundaries. The authors compared results on T_χ and μ_b deduced from various heavy-ion experiments with recent lattice simulations, effective QCD-like Polyakov

linear-sigma model, and equilibrium thermal model. Along the entire freezeout boundary, we conclude that an excellent agreement between the thermal model calculations and the experiments is found. Also, the estimations deduced from the Polyakov linear-sigma model excellently agree with the thermal model calculations. It should be noted that at low baryon density or high energies, both deconfinement and chemical freezeout boundaries are likely coincident. Accordingly, we can also conclude that the lattice calculations for the deconfinement transition agree well with the Polyakov linear-sigma model, where in both approaches QCD symmetries are included. At large baryon density or low energies, the two boundaries become distinguishable and probably form a phase in which hadrons and quark-gluon plasma likely coexist.

Based on the fact that Polyakov linear-sigma model agrees well with the lattice QCD simulations, at least within μ_b -range of reliable simulations, a future phenomenological study should be conducted on Polyakov linear-sigma model to find out whether the condition of line-of-constant-physics gives results in agreement with the $T_\chi - \mu_b$ plane for deconfinement. Furthermore, it intends to characterize the phase of mixed hadron-QGP and its possible predictions at the future facilities FAIR and NICA as well as its astrophysical consequences.

-
- [1] D. Parganlija, F. Giacosa, D. H. Rischke, P. Kovacs, and G. Wolf, *Int. J. Mod. Phys. A* **26**, 607 (2011).
 - [2] T. Banks and A. Ukawa, *Nucl. Phys. B* **225**, 145 (1983).
 - [3] A. N. Tawfik, *Int. J. Mod. Phys. A* **29**, 1430021 (2014).
 - [4] B. P. Abbott et al., *Phys. Rev. Lett.* **119**, 161101 (2017).
 - [5] M. Gyulassy and L. McLerran, *Nucl. Phys. A* **750**, 30 (2005).
 - [6] W. Busza, K. Rajagopal, and W. van der Schee, *Ann. Rev. Nucl. Part. Sci.* **68**, 339 (2018).
 - [7] C. Greiner, P. Koch-Steinheimer, F. M. Liu, I. A. Shovkovy, and H. Stoecker, *J. Phys. G* **31**, S725 (2005).
 - [8] B. Mueller and A. Schaefer, (2017).
 - [9] V. Vovchenko, M. I. Gorenstein, C. Greiner, and H. Stoecker, *Phys. Rev. C* **99**, 045204 (2019).
 - [10] L. D'Alessio, Y. Kafri, A. Polkovnikov, and M. Rigol, *Adv. Phys.* **65**, 239 (2016).
 - [11] G. Fast, R. Hagedorn, and L. W. Jones, *Nuovo Cim.* **27**, 856 (1963).
 - [12] G. Fast and R. Hagedorn, *Nuovo Cim.* **27**, 208 (1963).
 - [13] F. Karsch, K. Redlich, and A. Tawfik, *Eur. Phys. J. C* **29**, 549 (2003).
 - [14] F. Karsch, K. Redlich, and A. Tawfik, *Phys. Lett. B* **571**, 67 (2003).
 - [15] K. Redlich, F. Karsch, and A. Tawfik, *J. Phys. G* **30**, S1271 (2004).
 - [16] A. Tawfik, *Phys. Rev. D* **71**, 054502 (2005).
 - [17] A. Tawfik and D. Toublan, *Phys. Lett. B* **623**, 48 (2005).
 - [18] M. Tanabashi et al., *Phys. Rev. D* **98**, 030001 (2018).
 - [19] A. N. Tawfik and E. Abbas, *Phys. Part. Nucl. Lett.* **12**, 521 (2015).
 - [20] A. Tawfik, M. Y. El-Bakry, D. M. Habashy, M. T. Mohamed, and E. Abbas, *Int. J. Mod. Phys. E* **25**, 1650018 (2016).
 - [21] A. Tawfik, *Nucl. Phys. A* **764**, 387 (2006).
 - [22] A. Tawfik, *Europhys. Lett.* **75**, 420 (2006).
 - [23] A. Tawfik, *Nucl. Phys. A* **922**, 225 (2014).
 - [24] A. Tawfik, *Adv. High Energy Phys.* **2013**, 574871 (2013).
 - [25] A. Tawfik, *Phys. Rev. C* **88**, 035203 (2013).
 - [26] A. N. Tawfik, H. Yassin, and E. R. A. Elyazeed, *Phys. Rev. D* **92**, 085002 (2015).
 - [27] A. Tawfik, *J. Phys. G* **31**, S1105 (2005).
 - [28] V. I. Yukalova and E. P. Yukalov, *PoS Baldin-ISHEPP-XXI*, 046 (2012).
 - [29] V. A. Kizka, V. S. Trubnikov, K. A. Bugaev, and D. R. Oliinychenko, (2015).
 - [30] J. Beringer et al., *Phys. Rev. D* **86**, 010001 (2012).
 - [31] P. Man Lo, M. Marczenko, K. Redlich, and C. Sasaki, *Eur. Phys. J. A* **52**, 235 (2016).
 - [32] J. Noronha-Hostler, Implications of Missing Resonances in Heavy Ions Collisions, in *Workshop on Excited Hyperons in QCD Thermodynamics at Freeze-Out (YSTAR2016) Mini-Proceedings*, pages 118–127, 2016.
 - [33] S. Capstick and N. Isgur, *Phys. Rev. D* **34**, 2809 (1986), [AIP Conf. Proc.132,267(1985)].
 - [34] A. Bazavov et al., *Phys. Rev. Lett.* **113**, 072001 (2014).
 - [35] R. Bellwied et al., *Phys. Lett. B* **751**, 559 (2015).
 - [36] A. Bazavov et al., *Phys. Lett. B* **795**, 15 (2019).
 - [37] A. Tawfik, N. Magdy, and A. Diab, *Phys. Rev. C* **89**, 055210 (2014).
 - [38] O. Philipsen, Lattice QCD at non-zero temperature and baryon density, in *Modern perspectives in lattice QCD: Quantum field theory and high performance computing. Proceedings, International School, 93rd Session, Les Houches, France, August 3-28, 2009*, pages 273–330, 2010.
 - [39] A. Nasser Tawfik and A. Magied Diab, *Int. J. Mod. Phys. A* **30**, 1550059 (2015).